



Contents lists available at ScienceDirect

Tetrahedron Letters

journal homepage: [www.elsevier.com/locate/tetlet](http://www.elsevier.com/locate/tetlet)

# Synthesis and characterization of cyclophane: The highly selective recognition of $\text{Fe}^{3+}$ in aqueous solution and $\text{H}_2\text{PO}_4^-$ in acetonitrile solution

Ji Zhou<sup>a</sup>, Yao-Feng Yuan<sup>a,b,\*</sup>, Ji-Bin Zhuo<sup>a,c</sup>, Cai-Xia Lin<sup>a,\*</sup>

<sup>a</sup> Department of Chemistry, Fuzhou University, Fuzhou, Fujian 350116, China

<sup>b</sup> State Key Laboratory of Structural Chemistry, Fujian Institute of Research on the Structure of Matter, Chinese Academy of Sciences, Fuzhou, Fujian 350002, China

<sup>c</sup> Fuyuan Biotechnologies Co., Ltd., Fuzhou 350001, China

## ARTICLE INFO

### Article history:

Received 29 November 2017

Revised 16 January 2018

Accepted 2 February 2018

Available online xxx

### Keywords:

Cyclophane

Chemosensor

Hydrophilicity

Bathochromic-shift

$\text{Fe}^{3+}$  and  $\text{H}_2\text{PO}_4^-$

## ABSTRACT

In this work, we report a series of cyclophane fluorescent sensors based on acridine combining with imidazolium through ether linkages. X-ray crystal structures demonstrated the self-assembly behavior of these cyclophanes in the solid state driven by hydrogen bond and  $\pi$ - $\pi$  interactions. Sensors showed excellent selectivity towards  $\text{Fe}^{3+}$  in aqueous solution ( $\text{H}_2\text{O}/\text{CH}_3\text{CN} = 49:1, \text{v/v}$ ) and  $\text{H}_2\text{PO}_4^-$  in acetonitrile solution with notable color change under UV light, evident changes were also noticed in fluorescence spectra. In fluorescence emission, the obvious turn-off was induced by  $\text{Fe}^{3+}$  in aqueous solution and the obvious turn-on as well as bathochromic-shift was induced by  $\text{H}_2\text{PO}_4^-$  in acetonitrile solution.

© 2018 Elsevier Ltd. All rights reserved.

## Introduction

Design and synthesis of fluorescent chemosensors capable of selective recognition of ions is an active research field in supramolecular chemistry.<sup>1–4</sup> Ions play significant roles in chemical, biological, medical and environmental processes.<sup>5,6</sup> For example,  $\text{Fe}^{3+}$  is crucial to biological and environmental systems including cellular metabolism, oxidoreductase catalysis, oxygen transport, as well as DNA and RNA synthesis.<sup>7</sup> Abnormal  $\text{Fe}^{3+}$  fluctuations are often the cause of diseases, such as anemia, arthritis, heart failure, diabetes and cancer.<sup>8,9</sup> There are various analytical techniques such as atomic absorption spectroscopy, electrochemistry, spectrophotometry and inductively coupled plasma mass spectrometry that have been adopted for the determination of  $\text{Fe}^{3+}$ .<sup>10–13</sup> But these methods have self-defect factors such as sophisticated instrumentation, and complicated pretreatment procedures due to the poor anti-interference ability. Therefore, it is meaningful for us to design a specific ions sensor. Recently, fluorescence-based techniques have provided a simple, sensitive, selective, relatively low-cost method for online monitoring without

any pretreatment of the sample, the analytical technique have gained increasing attention for the detection of  $\text{Fe}^{3+}$ .<sup>14–19</sup> Moreover, hydrophilicity of sensors is essential for interfacing with biological substrates such as proteins and DNA etc.<sup>20</sup> Therefore for practical applications especially in biological system, it is necessary to develop  $\text{Fe}^{3+}$  chemosensors that are selective, possess good hydrophilicity and sensitive fluorescence signal output.<sup>20</sup> For example, Wang and Liu<sup>21</sup> reported three macrocyclic fluorescent sensors for  $\text{Fe}^{3+}$  ion and  $\text{Cu}^{2+}$  ion in the DMSO/ $\text{H}_2\text{O}$  solution, but the hydrophilicity and selectivity of sensors are not ideal.

From biological point of view,  $\text{H}_2\text{PO}_4^-$  is considered to be essential in metabolic process, signal transduction, energy storage, and construction of the backbone of DNA and RNA.<sup>22</sup>  $\text{H}_2\text{PO}_4^-$  have received extensive attention from chemists because of its unique properties, the response of the fluorescence employs a quenching or increase of the fluorescence for most of the reported  $\text{H}_2\text{PO}_4^-$  fluorescent sensors.<sup>23–25</sup> Indeed, some variable factors such as photobleaching, sensor molecular concentration and the microenvironment around the sensor molecules could also cause fluorescence quenching or enhancement in practical applications.<sup>23</sup> In contrast, the turn-on as well as the bathochromic-shift/hypochromic-shift of the fluorescence emission is a novel strategy for anion sensing.<sup>26,27</sup>

In these years, our group has been working hard at exploiting effective electrochemical and fluorescent detectors for ions.<sup>28–32</sup>

\* Corresponding authors at: Department of Chemistry, Fuzhou University, Fuzhou, Fujian 350116, China (Y.-F. Yuan).

E-mail addresses: [yaofeng\\_yuan@fzu.edu.cn](mailto:yaofeng_yuan@fzu.edu.cn) (Y.-F. Yuan), [lincaixia\\_fzu@fzu.edu.cn](mailto:lincaixia_fzu@fzu.edu.cn) (C.-X. Lin).

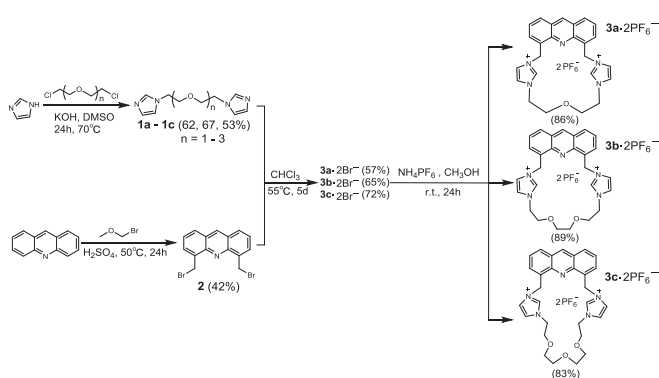
Most of our work focus on the design of imidazolium-based sensors, since this kind of functionalization sensors can be easily synthesized by reacting correspond imidazoles with a halogenate compound through the N atom of imidazole ring.<sup>33,34</sup> Additionally, imidazolium salt imply a higher hydrophilicity for the sensor, which means it's more likely to be applied in biological system.<sup>35–37</sup> During recent years, cyclophanes consist of a rigid aromatic unit and a flexible chain have become one of the most important kind of chemosensors due to their excellent performance in recognizing inorganic, organic cations, ions and neutral substrates selectively.<sup>38,39</sup>

The structure and rigidity of the sensors are important factors for ion sensing.<sup>5,6</sup> Cyclophane sensors performed better than their acyclic counterparts due to the well-preorganized topology.<sup>23</sup> In this work, we report a series of cyclophane fluorescent chemosensors **3a–3c**, which were constructed by acridine combining with imidazolium through ether linkages. The size of the sensors can be easily adjusted by changing the length of the ether linkage, and the oxygen atom can provide an recognition site for cations.<sup>40,41</sup> Moreover, the ether chain facilitates the hydrophilicity of sensor. As expected, sensors **3a–3c** showed specific response to  $\text{Fe}^{3+}$  in aqueous solution ( $\text{H}_2\text{O}/\text{CH}_3\text{CN} = 49:1, v/v$ ) with an apparent fluorescence quench. For  $\text{H}_2\text{PO}_4^-$ , sensors **3a–3c** showed an impressive bathochromic-shift behavior in their fluorescence spectra.

## Results and discussion

### Design and synthesis of the cyclophane sensors

As shown in Scheme 1, the synthesis of 4,5-bis(bromomethyl)acridine **2** was achieved by the reaction of acridine and bromomethylether at 50 °C in  $\text{H}_2\text{SO}_4$  with a 42% yield.<sup>23</sup> Bisimidazoles **1a–1c** were prepared by the reaction of 1,1'-oxybis(2-chloroethane), 1,2-bis(2-chloroethoxy)ethane and bis[2-(2-chloroethoxy)ethyl]ether with imidazole in the presence of KOH in DMSO at 70 °C for 24 h.<sup>42,43</sup> Then bisimidazoles **1a–1c** reacted with **2** in  $\text{CHCl}_3$  under high dilution conditions for 5 days to afford the bromide salts of sensors **3a–3c** in the yields of 57, 65 and 72%, respectively. Finally, a counterion exchange reaction using  $\text{NH}_4\text{PF}_6$  in methanol gave the desired hexafluorophosphate salts of sensors **3a–3c**. All the sensors **3a–3c** were characterized by  $^1\text{H}$  NMR,  $^{13}\text{C}$  NMR and HRMS.



Scheme 1. Synthesis of cyclophane sensors **3a–3c**.

### Crystal structures

Crystals of **3a-2PF<sub>6</sub><sup>-</sup>**, **3b-2PF<sub>6</sub><sup>-</sup>** and **3c-2PF<sub>6</sub><sup>-</sup>** suitable for X-ray diffraction studies were obtained from slow evaporation of con-

centrated solutions of the corresponding sensors in  $\text{CH}_3\text{OH}-\text{CH}_3\text{COCH}_3-\text{CH}_3\text{CN}$ .

The crystal structure of **3a** reveals that cyclophane adopts a cave-like conformation (Fig. 1). Two hydrogen atoms of the two imidazoliums pointed upward outside of the cavity and formed hydrogen bonds with fluorine atoms of one  $[\text{PF}_6]^-$  (2.30 Å). Adjacent molecules were connected by  $\pi$  stacking:  $\pi-\pi$  between two malposed acridine rings (3.653 Å). The crystal packing structure revealed the self-assembly nature of sensor **3a** in the solid state. Hydrogen bond and  $\pi-\pi$  stacking are major interactions for this assembly behavior. **3b** and **3c** is similar to that of **3a**, with the increase of the length of ether, the cavity size of **3b** is bigger than **3a** and ether structure of **3c** become distorted. From these crystal structures of sensors, some interesting points could be easily noticed. First, all the C(2) protons of the imidazoliums in these sensors were involved in hydrogen bonds with counterions, indicating their potential binding abilities for other competitive anions. Then, all the sensors **3a–3c** presented a cave-like conformation in which two C(2)-H of imidazoliums pointed upward outside of the cavity. This conformation would facilitate the two imidazoliums binding an anion which has two bifurcated electronegative atoms, such as  $\text{H}_2\text{PO}_4^-$ , with a good preorganization.<sup>23</sup> Finally, all the sensors showed a self-connected network in the solid state driven by hydrogen bond and  $\pi-\pi$  interactions. Especially, we observed the obvious but different extent  $\pi-\pi$  interactions between two acridine rings in the crystal structures of these sensors. The formation of the acridine dimers to a different extent could result in different

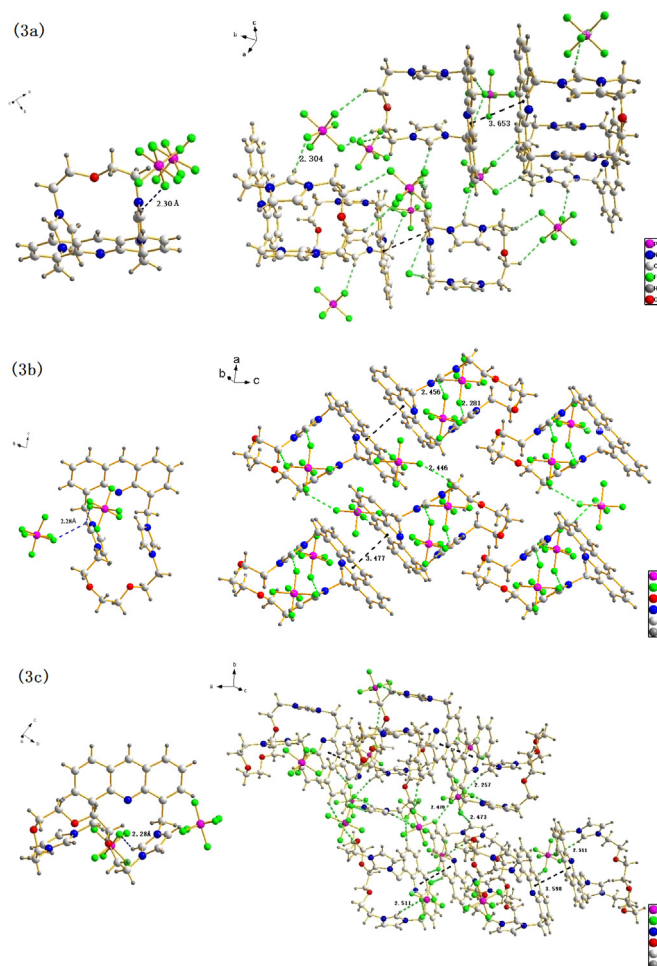


Fig. 1. Crystal structure and the self-assembly network of **3a–3c-2(PF<sub>6</sub><sup>-</sup>)**. Dashed lines represent hydrogen bonds and  $\pi-\pi$  interactions.

bathochromic-shifts of the fluorescence emission if occurred in solution,<sup>44–46</sup> which would promote the understanding of the following anion-induced assembly-based fluorescence sensing of anions in solution.

### Fe<sup>3+</sup>-induced fluorescence decrease in fluorescence emission

A series of metal ions were used to evaluate the binding properties. As presented in Fig. 2, the studies for the interaction between sensors **3a–3c** (10 μM) and various metal ions such as Zn<sup>2+</sup>, Al<sup>3+</sup>, Cd<sup>2+</sup>, Co<sup>2+</sup>, Cr<sup>3+</sup>, Cu<sup>2+</sup>, Hg<sup>2+</sup>, Mg<sup>2+</sup>, Mn<sup>2+</sup>, Na<sup>+</sup>, Ni<sup>2+</sup>, Pb<sup>2+</sup> and Fe<sup>3+</sup> (1 mM) were monitored clearly by the fluorescence spectroscopy in aqueous solution (H<sub>2</sub>O/CH<sub>3</sub>CN = 49:1, v/v).

The addition of Fe<sup>3+</sup> created a remarkable fluorescence decrease, while addition of the same amount of other metal ions displayed negligible fluorescence responses. In addition, for an excellent probe, first consideration should be given to the high selectivity, so the selectivity and anti-interference performance of sensors **3a–3c** (Fig. 2) were explored in the presence of cations of interest. The addition of Fe<sup>3+</sup> (1 mM) to the solutions of sensors **3a–3c** (10 μM) with interfering cations (1 mM) appeared similar decrease that caused by Fe<sup>3+</sup> only. These results indicated that the specific responses of sensors **3a–3c** to Fe<sup>3+</sup> were not disturbed by other competitive cations. We can see clearly in Fig. 2, the fluorescence intensity of sensor **3b** is higher than that of sensors **3a** and **3c**.

To get an insight into the sensing properties of sensors **3a–3c** to Fe<sup>3+</sup>, fluorescence titration experiments were then performed. As shown in Fig. 3, upon incremental addition of Fe<sup>3+</sup> to sensors solution, the fluorescence emission gradually decreased and reached the saturation state when 100 equiv. of Fe<sup>3+</sup> ion was employed, which suggested that there would be certain interaction between sensors and Fe<sup>3+</sup>. This mechanism could be attributed to the formation of a rigid system after binding with Fe<sup>3+</sup>, causing the photoin-

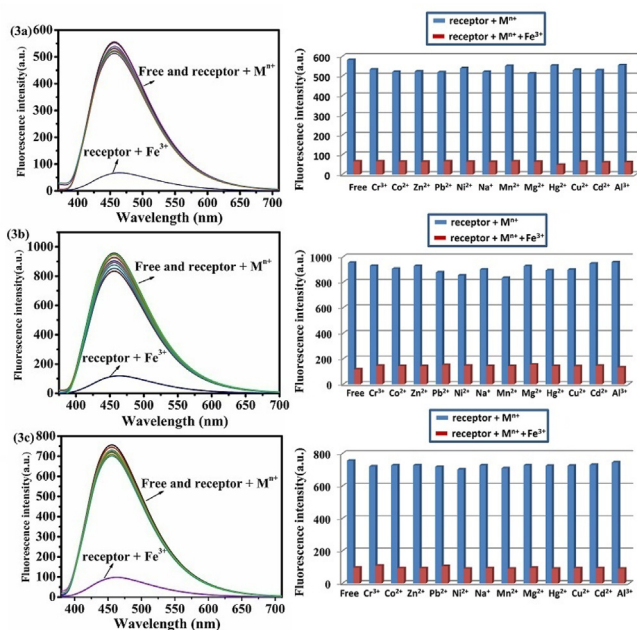


**Fig. 2.** Left: Changes in the emission spectrum of **3a–3c** (10 μM) in the presence of different metal ions (1 mM) in aqueous solution (H<sub>2</sub>O/CH<sub>3</sub>CN = 49:1, v/v), excited at 360, 360 and 365 nm respectively; Right: Fluorescence responses of **3a–3c** (10 μM) to Fe<sup>3+</sup> (1 mM) in the presence of other common metal ions (1 mM). The blue bars represent the fluorescence intensity of **3a–3c** in the presence of cations of interest (1 mM). The red bars represent the changes of the emission that occurs upon the subsequent addition of 1 mM of Fe<sup>3+</sup> to the above solution. Emission at 455 nm (excitation and emission slit: 2.5 nm and 5 nm).

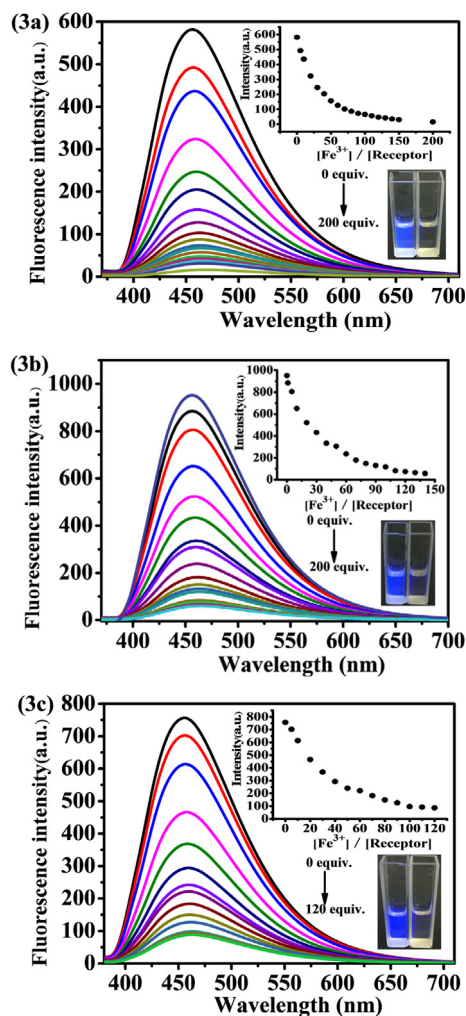


**Fig. 3.** Fluorescence titrations of 10 μM sensor **3a** excited at 360 nm, **3b** excited at 360 nm and **3c** excited at 365 nm with Fe<sup>3+</sup> in aqueous solution (H<sub>2</sub>O/CH<sub>3</sub>CN = 49:1, v/v) (excitation and emission slit: 2.5 nm and 5 nm).

duced electron transfer (PET) effect.<sup>47–49</sup> The fluorescence data revealed that the binding of sensors **3a–3c** to Fe<sup>3+</sup> was most probably of 1:1 stoichiometry. The binding mode was also supported by the data of Job's plots<sup>50</sup> evaluated from the emission spectra of sensors **3a–3c** and Fe<sup>3+</sup> with a total concentration of 10 μM (Fig. S33). According to linear Benesi-Hildebrand expression, the measured fluorescence intensity  $[1/(F - F_0)]$  varied as a function of  $1/[Fe^{3+}]$  in a linear relationship ( $R^2$  are 0.9968, 0.9914 and 0.9976 respectively). This binding mode was also supported by the data of Benesi-Hildebrand (Figs. S27–29).<sup>51</sup> The association constant of sensors **3a–3c** with Fe<sup>3+</sup> in aqueous solutions were accordingly calculated to be  $2.907 \times 10^3 \text{ M}^{-1}$ ,  $3.094 \times 10^3 \text{ M}^{-1}$  and  $2.459 \times 10^3 \text{ M}^{-1}$ , respectively. The detection limit for Fe<sup>3+</sup> was estimated to be  $1.88 \times 10^{-5} \text{ M}$  (1.049 mg/L),  $4.43 \times 10^{-6} \text{ M}$  (0.247 mg/L) and  $8.28 \times 10^{-6} \text{ M}$  (0.462 mg/L) respectively based on a  $3\sigma/\text{slope}$  analysis under these experimental conditions (Figs. S34–36).<sup>52</sup> The detection limit of **3b** is lower than the maximum permitted amount of Fe<sup>3+</sup> (0.3 mg/L) in drinking water defined by the U.S Environmental Protection Agency (EPA),<sup>53</sup> implying that sensor **3b** holds great potential for the development of sensor materials for Fe<sup>3+</sup>. The emission color change from blue to colorless can be clearly observed under UV light in presence of Fe<sup>3+</sup>.

It is to be noted that sensors **3a–3c** shows high selectivity for Fe<sup>3+</sup> ion. It is well-known that heavy metal ions tend to quench the luminescence through electron-transfer and/or energy-transfer

processes.<sup>54,55</sup> The fluorescent turn-off response maybe caused by the formation of the complex between sensors **3a–3c** and  $\text{Fe}^{3+}$  ion. The HOMO energy level of  $\text{Fe}^{3+}$  ion was between the HOMO and LUMO energy levels of the fluorophore units. When  $\text{Fe}^{3+}$  conjugated with sensors **3a–3c**, after excited by the light, the partly filled orbitals of  $\text{Fe}^{3+}$  would readily to accept the electrons from delocalised-electron system of sensors **3a–3c**.<sup>21</sup> Thus, the photoinduced electron transfer (PET) effect caused the fluorescence quenching of acridine.<sup>56–60</sup>

#### $\text{H}_2\text{PO}_4^-$ -induced bathochromic-shift in fluorescence emission

In order to investigate the corresponding anion-binding properties in solution, the studies of the interaction between sensors **3a–3c** ( $5\ \mu\text{M}$ ) and a series of anions such as  $\text{F}^-$ ,  $\text{Cl}^-$ ,  $\text{Br}^-$ ,  $\text{I}^-$ ,  $\text{HSO}_4^-$ ,  $\text{AcO}^-$ ,  $\text{OH}^-$ ,  $\text{ClO}_4^-$  and  $\text{H}_2\text{PO}_4^-$  ( $50\ \mu\text{M}$ ) were evaluated by fluorescence spectra upon addition of various anions to the  $\text{CH}_3\text{CN}$  solutions of **3a–3c**. Tetrabutylammonium (TBA<sup>+</sup>) salts of various anions were used since their negligible supramolecular interactions to most reported sensors.<sup>23</sup> As presented in Fig. 4, in the absence of anions, the fluorescence spectra of sensors **3a–3c** all showed a peak at about 450 nm, corresponding to the blue fluorescence. The addition of  $\text{H}_2\text{PO}_4^-$  created a remarkable bathochromic-shift and a negligible fluorescence response was observed upon the addition of the same amount of other anions, which suggested that there would be certain interaction between sensors **3a–3c** and  $\text{H}_2\text{PO}_4^-$ . This phenomenon could be attributed to the  $\text{H}_2\text{PO}_4^-$ -induced assembly of sensors **3a–3c** forming the excimer conformation between two acridine rings, causing the Excimer/Exciplex effect.<sup>44–46,61,62</sup> Achieving high selectivity toward  $\text{H}_2\text{PO}_4^-$  over the other competitive species coexisting was a very important feature to evaluate the performance of sensors. Therefore, the competition experiments were also conducted for sensors. Fig. 4 indicated that when  $\text{H}_2\text{PO}_4^-$  were added into the solution of sensors in the pres-

ence of other ions, the emission spectra displayed a similar pattern to that with  $\text{H}_2\text{PO}_4^-$  only.

The further fluorescence titration experiments of sensors **3a–3c** with  $\text{H}_2\text{PO}_4^-$  were performed as shown in Fig. 5. Upon incremental addition of  $\text{H}_2\text{PO}_4^-$  (0–10 equiv.) to the sensors  $\text{CH}_3\text{CN}$  solution, significant decrease was observed in their emission spectra at 450, 434 and 450 nm, respectively, accompanying an increase of bathochromic-shift emission band clearly at 527, 515 and 520 nm, respectively. Take sensor **3b** as example, a clear “turn-off” of fluorescence emission at 434 nm and an apparent “turn-on” of fluorescence emission at 515 nm were observed upon addition of 4 equiv. of  $\text{H}_2\text{PO}_4^-$ , obvious bathochromic-shifts of fluorescence emission were observed. Interestingly, the wavelengths of the excimer emission induced by  $\text{H}_2\text{PO}_4^-$  for different sensors were distinctly different, and the bathochromic-shifts of sensors **3a–3c** in fluorescence emission are 77, 81 and 70 nm, respectively. The different bathochromic-shift emission for different sensors might be attributed to the formation of the excimer conformation to a different extent.<sup>44–46</sup> The emission color change from blue to yellow-green can be clearly observed under UV light in the presence of  $\text{H}_2\text{PO}_4^-$  that is the alignment with the fluorescent spectra. It is noteworthy that the intensity of the bathochromic-shift emission bands was higher than those of the original peaks at the end of the titrations

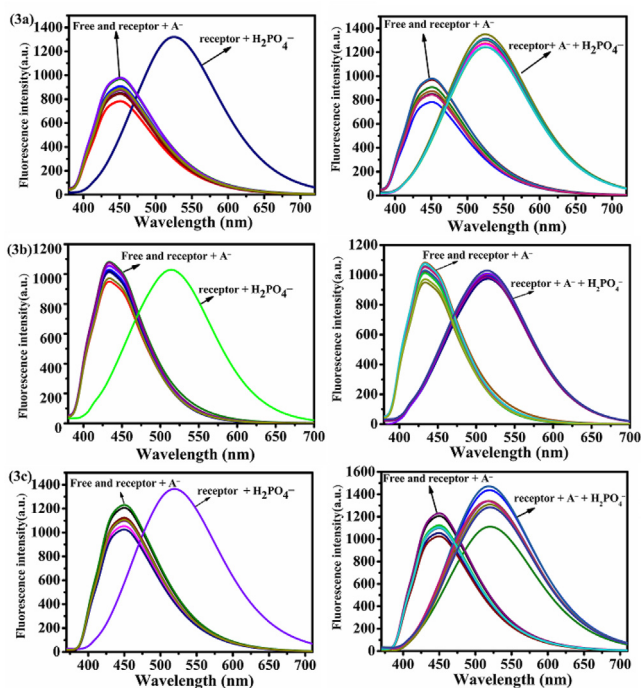


**Fig. 4.** Left: Changes in the emission spectrum of **3a–3c** ( $5\ \mu\text{M}$ ) in the presence of different anions ( $50\ \mu\text{M}$ ) in  $\text{CH}_3\text{CN}$ ; Right: Fluorescence responses of **3a–3c** ( $5\ \mu\text{M}$ ) in the presence of different anions ( $50\ \mu\text{M}$ ) and Fluorescence responses of **3a–3c** ( $5\ \mu\text{M}$ ) to  $\text{H}_2\text{PO}_4^-$  ( $50\ \mu\text{M}$ ) in the presence of other common anions ( $50\ \mu\text{M}$ ) in  $\text{CH}_3\text{CN}$ . Excited at 365, 365 and 360 nm respectively. (excitation and emission slit: 5 nm).

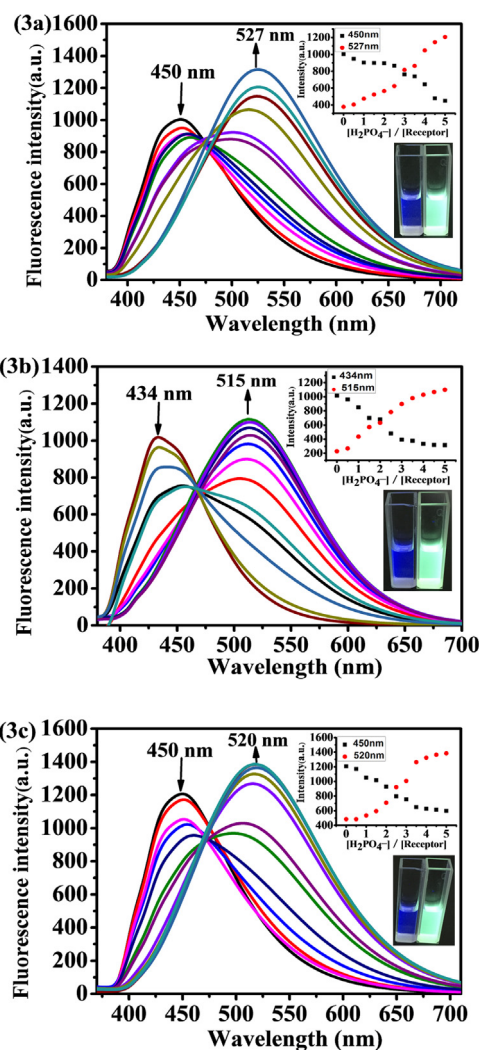
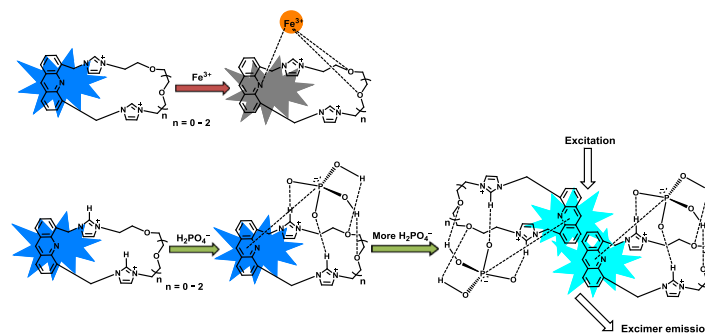


**Fig. 5.** Fluorescence titrations of  $5\ \mu\text{M}$  sensors **3a** excited at 365 nm, **3b** excited at 365 nm and **3c** excited at 360 nm with  $\text{TBAH}_2\text{PO}_4$  in  $\text{CH}_3\text{CN}$ . (excitation and emission slit: 5 nm).



**Scheme 2.** The proposed mechanism for  $\text{Fe}^{3+}$  and  $\text{H}_2\text{PO}_4^-$  detection by sensors.

for all the sensors, demonstrating that the bathochromic-shift of the fluorescence emission induced by  $\text{H}_2\text{PO}_4^-$  for all the sensors was rather validated and reliable. The results exhibited that the course of titrations for all the sensors may contain a two-step process, which were most likely due to the  $\text{H}_2\text{PO}_4^-$  complexation with one sensor molecule firstly, and then followed by the  $\text{H}_2\text{PO}_4^-$ -induced assembly of sensors forming the acridine dimer at a higher concentration of  $\text{H}_2\text{PO}_4^-$ .<sup>23</sup> Job's plot<sup>50</sup> revealed the equal ratio stoichiometric complexes of sensors **3a–3c** with  $\text{H}_2\text{PO}_4^-$ . This binding mode was also supported by the data of Job's plots evaluated from the emission spectra of sensors **3a–3c** and  $\text{H}_2\text{PO}_4^-$  with a total concentration of  $5 \mu\text{M}$  (Fig. S33). The association constant of sensors **3a–3c** with  $\text{H}_2\text{PO}_4^-$  in  $\text{CH}_3\text{CN}$ , as determined from fluorescence titrations, was accordingly calculated to be  $2.56 \times 10^4$ ,  $5.37 \times 10^4$  and  $2.15 \times 10^4 \text{ M}^{-1}$  respectively (Figs. S30–32).<sup>63</sup> The detection limit for  $\text{H}_2\text{PO}_4^-$  was estimated to be  $5.03 \times 10^{-7}$ ,  $2.89 \times 10^{-7}$  and  $2.13 \times 10^{-7} \text{ M}$  respectively based on a  $3\sigma/\text{slope}$  analysis by using the fluorescence titration results (Figs. S34–36).<sup>52</sup>

Notably, the  $\text{H}_2\text{PO}_4^-$  titration results in  $\text{CH}_3\text{CN}$  for all the sensors **3a–3c** followed the rule: with the increase of the ether length, the induced bathochromic-shift of emission regularly increased then decreased, anti-interference performance of the sensor **3c** get worse for anions. The performance of sensors **3b** is the best one. Sensor **3b** exhibited a  $\pi$ - $\pi$  interaction between two acridines with the largest extent induced by  $\text{H}_2\text{PO}_4^-$ , which may be because the cavity size and macrocyclic rigidity effects of sensor **3b** is the just right leading to the largest stabilization energy in the excited state and the largest repulsion energy in the ground state.<sup>44</sup> But beyond that, because of the “turn-on” and quantitative bathochromic-shift of their fluorescence emission, the sensor **3a–3c** could be used as highly selective ratiometric fluorescent sensors for  $\text{H}_2\text{PO}_4^-$  in  $\text{CH}_3\text{CN}$ .<sup>23</sup>

We further attempted to investigate the fluorescence emission of sensor **3b** ( $10 \mu\text{M}$ ) in aqueous media (Fig. S23). The excimer peaks were still visible in the presence of 1% water upon addition of  $\text{TBAH}_2\text{PO}_4$ . However, the bathochromic-shifts completely disappeared in the presence of 2.5% water, which could be attributed to the influence of hydrogen bonding interaction of water with anions.<sup>64</sup>

To explore the mechanism underlying the detection of  $\text{H}_2\text{PO}_4^-$  and  $\text{Fe}^{3+}$  by sensors **3a–3c**.  $^1\text{H}$  NMR titration experiments (Fig. S37) were carried out in  $\text{CD}_3\text{CN}$  between sensors **3a–3c** ( $5 \text{ mM}$ ) and  $\text{H}_2\text{PO}_4^-$ . As expected, upon addition of 1.5 equiv. of  $\text{H}_2\text{PO}_4^-$  to the solution of sensors **3a–3c** ( $5 \text{ mM}$ ), 0.03, 0.08 and 0.06 ppm downfield shift was observed for C(2)-H of imidazolium respectively, clearly suggesting the sensor-anion complexation by hydrogen bonds. The precipitation was observed with progressive addition of  $\text{H}_2\text{PO}_4^-$ . However, upfield shifts of the aromatic protons of the acridine ring still were observed, especially sensors **3a**, which demonstrated the formation of the face-to-face  $\pi$ - $\pi$  interaction between two anthracenes.<sup>65</sup> In addition, downfield shifts of the ether protons were also observed, demonstrating the formation

of hydrogen bonds between  $\text{H}_2\text{PO}_4^-$  and the oxygen atom of ether.<sup>66</sup> (Fig. S37). The proposed mechanism for the  $\text{H}_2\text{PO}_4^-$  and  $\text{Fe}^{3+}$  detection was further supported by the results of mass spectra studies. As shown in Fig. S18. HRMS spectra of sensors showed molecular-ion peak ( $\text{M}+\text{PF}_6^-$ ) at  $m/z$  556.1678, 600.1979 and 644.2197 respectively,  $\text{M}/2$  at  $m/z$  205.6018, 227.6163 and 249.6280 respectively (Fig. S17). When the  $\text{Fe}^{3+}$  ion was added into the solution of sensors **3a–3c**, the peak at  $m/z$  609.06, 653.08 and 697.15 were assigned to ( $\text{M}+\text{PF}_6^-+\text{Fe}^{3+}-2\text{H}^+$ ) species (Fig. S18). It's notably that after addition 100 eqv mole of  $\text{Na}_2\text{S}_2\text{O}_3$ , the signal for ( $\text{M}+\text{PF}_6^-+\text{Fe}^{3+}-2\text{H}^+$ ) almost disappeared (Fig. S19), which verified the selectivity for  $\text{Fe}^{3+}$ . For  $\text{H}_2\text{PO}_4^-$ , when the  $\text{H}_2\text{PO}_4^-$  ion was added into the solution of sensors **3a–3c**, the peak at  $m/z$  508.21, 552.27 and 596.72 were assignable to ( $\text{M}+\text{H}_2\text{PO}_4^-$ ) species (Fig. S18). This result confirmed that 1:1 stoichiometry complex between sensors **3a–3c** and  $\text{Fe}^{3+}/\text{H}_2\text{PO}_4^-$ .

The possible binding modes of these cyclophane sensors with  $\text{H}_2\text{PO}_4^-$  and  $\text{Fe}^{3+}$  were proposed by the discussions above of X-ray crystal structures, fluorescence spectra, mass spectra and  $^1\text{H}$  NMR titration. As shown in Scheme 2, due to the directional properties of the two partially charged oxygen atoms in  $\text{H}_2\text{PO}_4^-$ , the  $\text{H}_2\text{PO}_4^-$  anion formed hydrogen bonds with the two hydrogen atoms of imidazolium in the macrocyclic sensor with a 1:1 stoichiometry, corresponding to the fluorescence quenching due to the PET process. However, at a higher concentration of  $\text{H}_2\text{PO}_4^-$ , intermolecular  $\pi$ - $\pi$  stacking interactions between two acridine fluorophores were reinforced owing to the  $\text{H}_2\text{PO}_4^-$  induced assembly of sensors, thus a distinct excimer emission appeared and increased.<sup>65,66</sup> In addition, due to the effect of the varying bridged linkages between two imidazoliums, the bathochromic-shifts of fluorescence emission induced by  $\text{H}_2\text{PO}_4^-$  for sensors **3a–3c** were different.<sup>44</sup>

## Conclusions

In conclusion, we have developed a series of acridine-based imidazolium cyclophanes fluorescent chemosensor for  $\text{Fe}^{3+}$  in aqueous solution ( $\text{H}_2\text{O}/\text{CH}_3\text{CN} = 49:1, \text{v/v}$ ) and  $\text{H}_2\text{PO}_4^-$  in  $\text{CH}_3\text{CN}$ . Receptors showed excellent selectivity and sensitivity for recognizing  $\text{Fe}^{3+}$  and  $\text{H}_2\text{PO}_4^-$ , accompanying obvious color change. The ion-induced fluorescent emission of the sensors could be regulated by adjusting the ring size and rigidity. The assembly behavior of these sensors was demonstrated by X-ray crystal structures. These results are very encouraging, we recognize that further study is required to build upon this basis.

## Acknowledgement

This work was supported financially by the National Natural Science Foundation of China (Grant No. 21372043).

## A. Supplementary data

Supplementary data associated with this article can be found, in the online version, at <https://doi.org/10.1016/j.tetlet.2018.02.005>.

## References

- Zhao B, Xu Y, Deng Q, et al. *Tetrahedron Lett.* 2016;57:953–958.
- Chandrasekhar V, Das S, Yadav R, et al. *Inorg Chem.* 2012;51:8664–8866.
- Zhang JF, Zhou Y, Yoon J, Kim JS. *Chem Soc Rev.* 2011;40:3416–3429.
- Huo FJ, Yin CX, Yang YT, Su J, Chao JB, Liu DS. *Anal Chem.* 2012;84:2219–2223.
- Kim JS, Quang DT. *Chem Rev.* 2007;107:3780–3799.
- Duke RM, Veale EB, Pfeffer FM, Kruger PE, Gunnlaugsson T. *Chem Soc Rev.* 2010;39:3936–3953.
- Aisen P, Wessling-Resnick M, Leibold EA. *Curr Opin Chem Biol.* 1999;3:200–206.
- Narayanaswamy N, Govindaraju T. *Sens Actuators B.* 2012;161:304–310.
- Xu JH, Hou YM, Ma QJ, Wu XF, Wei XJ. *Spectrochim Acta A Mol Biomol Spectrosc.* 2013;112:116–124.
- Ohashi A, Ito H, Kanai C, Imura H, Ohashi K. *Talanta.* 2005;65:525–530.
- Akatsuka K, McLaren JW, Lam JW, Berman SS. *J Anal Atomic Spectrom.* 1992;7:889–894.
- Elrod VA, Johnson KS, Coale KH. *Anal Chem.* 1991;63:893–898.
- Tesfaldet ZO, van Staden JF, Stefan RI. *Talanta.* 2004;65:1189–1195.
- Valeur B, Leray I. *Coord Chem Rev.* 2000;205:3–40.
- Petrat F, Rauen U, De Groot H. *Hepatology.* 1999;29:1171–1179.
- Li P, Ji C, Ma H, Zhang M, Cheng Y. *Chem Eur J.* 2014;20:5741–5745.
- Zhang G, Lu B, Wen Y, Lu L, Xu J. *Sens Actuators B.* 2012;171:786–794.
- Qu X, Liu Q, Ji X, Chen H, Zhou Z, Shen Z. *Chem Commun.* 2012;48:4600–4602.
- Wu X, Xu B, Tong H, Wang L. *Macromolecules.* 2010;43:8917–8923.
- Jin L, Liu C, An N, et al. *RSC Adv.* 2016;6:58394–58400.
- Dai YP, Liu XY, Wang P. *Supramol Chem.* 2016;29:315–322.
- Saenger W. *Principles of Nucleic Acid Structure.* New York: Springer; 1988.
- Zhang D, Jiang X, Yang H, et al. *Org Biomol Chem.* 2013;11:3375–3381.
- Jadhav JR, Bae CH, Kim HS. *Tetrahedron Lett.* 2011;52:1623–1627.
- Lee GW, Singh N, Jung HJ, Jang DO. *Tetrahedron Lett.* 2009;50:807–810.
- Xu Z, Xiao Y, Qian X, Cui J, Cui D. *Org Lett.* 2005;7:889–892.
- Zhang D, Cochrane JR, Martinez A, Gao G. *RSC Adv.* 2014;4:29735–29749.
- Su ZM, Ye HM, Zhu XX, Xie LL, Bai S, Yuan YF. *J Organomet Chem.* 2014;750:162–168.
- Zhuo JB, Zhu XX, Lin CX, Bai S, Xie LL, Yuan YF. *J Organomet Chem.* 2014;770:85–93.
- Zhuo JB, Zhang CY, Lin CX, Bai S, Xie LL, Yuan YF. *J Organomet Chem.* 2014;763:34–43.
- Su ZM, Lin CX, Zhou YT, Xie LL, Yuan YF. *J Organomet Chem.* 2015;788:17–26.
- Wan Q, Zhuo JB, Wang XX, Lin CX, Yuan YF. *Dalton Trans.* 2015;44:5790–5796.
- Storch J, Zadny J, Strasak T. *Chem Eur J.* 2015;21:2343–2347.
- D'Anna F, Noto R. *Eur J Org Chem.* 2014;20:4201–4223.
- Xu Z, Singh NJ, Lim J. *J Am Chem Soc.* 2009;131:15528–15533.
- Xu Z, Kim SK, Yoon J. *Chem Soc Rev.* 2010;39:1457–1466.
- Ahmed N, Shirinfar B, Youn IS. *Chem Commun.* 2012;48:2662–2664.
- Wessjohann LA, Rivera DG, Vercillo OE. *Chem Rev.* 2009;109:796–814.
- Hopf H. *Angew Chem Int Ed.* 2008;47:9808–9812.
- Singh A, Singh N. *Tetrahedron.* 2016;72:3535–3541.
- Lin CX, Guo L, Li QS, Zhang ZZ, Yuan YF, Xu FB. *J Organomet Chem.* 2014;749:180–187.
- Eshghi H, Rahimizadeh M, Hasanpour M, Bakavoli M. *Res Chem Intermed.* 2015;41:4187–4197.
- Bara JE. *Ind Eng Chem Res.* 2011;50:13614–13619.
- Nakamura Y, Yamazaki T, Nishimura J. *Org Lett.* 2005;7:3259–3262.
- Shahid M, Razi SS, Srivastava P, Ali R, Maiti B, Misra A. *Tetrahedron.* 2012;68:9076–9084.
- Otabe T, Matsumoto S, Nakagawa H, Hong C, Dohno C, Nakatani K. *Tetrahedron Lett.* 2013;54:143–146.
- Kaur M, Kaur P, Dhuna V. *Dalton Trans.* 2014;43:5707–5712.
- Woodford CR, Frady EP, Smith RS, et al. *J Am Chem Soc.* 2015;137:1817–1824.
- Zhao X, Yin G, Jin D, Yan X, Li Y, Chen L. *J Fluoresc.* 2015;25:327–333.
- Job P. *Ann Chim.* 1928;9:113–203.
- Benesi HA, Hildebrand JH. *J Am Chem Soc.* 1949;71:2703–2707.
- Shiraishi Y, Sumiya S, Hirai T. *Chem Commun.* 2011;47:4953–4955.
- Mirlohi S, Dietrich AM, Duncan SE. *Environ Sci Technol.* 2011;45:6575–6583.
- Bricks JL, Kovalchuk A, Trieflinger C, et al. *J Am Chem Soc.* 2005;127:13522–13529.
- Kavallieratos K, Rosenberg JM, Chen WZ, Ren T. *J Am Chem Soc.* 2005;127:6514–6515.
- de Silva AP, Gunaratne HQN, Gunnlaugsson T, et al. *Pure Appl Chem.* 1996;68:1443–1448.
- de Silva AP. *Nat Chem.* 2012;4:440–441.
- Valeur B, ed. *Molecular Fluorescence.* Weinheim: Wiley-VCH; 2002:90–94.
- Jung HS, Kwon PS, Lee JW, et al. *J Am Chem Soc.* 2009;131:2008–2012.
- Villata LS, Wolcan EM, Feliz R, Capparelli AL. *J Phys Chem A.* 1999;103:5661–5666.
- Nishizawa S, Kato Y, Teramae N. *J Am Chem Soc.* 1999;121:9463–9464.
- Gong W, Zhang Q, Wang F, Gao B, Lin Y, Ning G. *Org Biomol Chem.* 2012;10:7578–7583.
- Ahmed N, Shirinfar B, Youn IS, Kim KS. *Org Biomol Chem.* 2013;11:6407–6413.
- Yuan Y, Gao G, Jiang ZL, et al. *Tetrahedron.* 2002;58:8993–8999.
- Zhang D, Jiang X, Yang H, Martinez A, Gao G. *Chem Commun.* 2013;49:6149–6151.
- Mahapatra AK, Hazra G, Sahoo P. *Bioorg Med Chem Lett.* 2012;22:1358–1364.